Journal of Electroanalytical Chemistry 886 (2021) 115113

Contents lists available at ScienceDirect

Journal of Electroanalytical Chemistry

journal homepage: www.elsevier.com/locate/jelechem

# Study on the electrochromic properties of polypyrrole layers doped with different dye molecules

Maryam Bayat [a], Hossein Izadan [a,*], Sara Santiago [b], Francesc Estrany [c,d], Mohammad Dinari [e], Dariush Semnani [a], Carlos Alemán [c,d,*], Gonzalo Guirado [b,*]

[a] Department of Textile Engineering, Isfahan University of Technology, Isfahan 84156-83111, Iran
[b] Departament de Química, Universitat Autònoma de Barcelona, 08193 Barcelona, Cerdanyola del Vallès, Spain
[c] Departament d'Enginyeria Química, EEBE, Universitat Politècnica de Catalunya, C/ Eduard Maristany 10-14, Ed. I2, 08019 Barcelona, Spain
[d] Barcelona Research Center for Multiscale Science and Engineering, Universitat Politècnica de Catalunya, Eduard Maristany 10-14, 08019 Barcelona, Spain
[e] Department of Chemistry, Isfahan University of Technology, Isfahan 84156-83111, Iran

ARTICLE INFO

*Keywords:*
Polypyrrole
Electrochromic
Spectroelectrochemical
Dye molecules
Dopant

ABSTRACT

Three dye molecules (Dye) of Acid Brilliant Scarlet 3R (AR18), Amido Naphthol Red G (AR1), Indigo Carmine (IC), as well as sodium dodecyl sulfate (SDS) as dopant agents were used for electrochemical synthesis of polypyrrole (PPy) layers onto indium doped tin oxide (ITO) coated polyethylene terephthalate (PET) electrode. The morphology, electrochemical, optical, and spectroelectrochemical properties of the layers were investigated. The study of the electrochemical behavior showed that the presence of each AR18, AR1, or IC with SDS, had shown an excellent synergistic effect on the electrochemical stability of layers. The morphological characterization of the PPy/dopant(s) using atomic force microscopy (AFM) showed that the surface roughness in the PPy/IC-SDS layer was 39% and 32% less than the PPy/AR18-SDS and PPy/AR1-SDS, respectively. The absorption spectrum of PPy/dopant(s) in the UV–Vis-NIR wavelength range showed the formation of polaron and bipolaron in PPy chains. Also, the optical bandgap energy of PPy/dopant(s) decreased, and the fully doped state in all PPy films was observed. Spectroelectrochemical properties of the films showed that the simultaneous use of each dye molecule and the surfactant as dopant in PPy layers demonstrated proper electrochemical and optical stability and satisfactory electrochromic parameters. For example, the color contrast of PPy/AR18-SDS was 50%, while this parameter in control sample (PPy doped with lithium perchlorate) was 21%. Also, the cathodic and anodic coloration efficiency showed a 6-fold increase in PPy/Dye-SDS compared to PPy/$ClO_4$. In general, according to the results it is likely that by increasing the number of anion groups in the dye molecules and decreasing their dimensions as dopant agents, the electrochemical and electrochromic properties of the resultant layer would be improved.

## 1. Introduction

Electrochromism is a process in which an electroactive material changes its color due to electron transfer (oxidation/reduction). Materials that are capable of reversible color change due to the application of external potential are called electrochromic materials [1]. Platt in 1961 stated for the first time that a color shift of hundreds of angstroms in some dyes is also possible when applying an external electric potential [2]. Electrochromic materials can be classified into three main categories according to their solubility of their redox states: solution electrochromes, solution-solid electrochromes, and solid electrochromes. In the first group, are the compounds that both states, the initial and the oxidized or reduced state, are soluble in the electrolyte during the color switching. In the second group, one of the states is insoluble while the other dissolves in the media. In the third type, the materials are solid in both oxidation states that is to say, before and after applying a voltage. A wide range of inorganic and organic chemicals are used in electrochromic processes, including but not limited to inorganic oxides, Prussian Blue, metal hexacyanometallates, metal phthalocyanines, viologens, and polymers [1,3].

* Corresponding authors at: Department of Textile Engineering, Isfahan University of Technology, Isfahan 84156-83111, Iran (H. Izadan); Departament d'Enginyeria Química, EEBE, Universitat Politècnica de Catalunya, C/ Eduard Maristany 10-14, Ed. I2, 08019 Barcelona, Spain (C. Alemán); Departament de Química, Universitat Autònoma de Barcelona, 08193 Barcelona, Cerdanyola del Vallès, Spain (G. Guirado).

*E-mail addresses:* maryam.bayat@alumni.iut.ac.ir (M. Bayat), izadan@iut.ac.ir (H. Izadan), sara.santiago@uab.cat (S. Santiago), francesc.estrany@upc.edu (F. Estrany), dinari@iut.ac.ir (M. Dinari), d_semnani@iut.ac.ir (D. Semnani), carlos.aleman@upc.edu (C. Alemán), gonzalo.guirado@uab.cat (G. Guirado).

https://doi.org/10.1016/j.jelechem.2021.115113
Received 12 January 2021; Received in revised form 14 February 2021; Accepted 22 February 2021
Available online 9 March 2021

Electrochromic polymers are a group of conducting polymers that are capable of color change under external voltage. These include polyaniline, polypyrrole (PPy), polyfuran, polycarbazole, and polythiophene derivatives [1,3–6]. Electrochromic polymers have achieved significance, in part because of their easy control of formation by spin coating, self-assembly, drop casting or electropolymerization techniques, among others, to form solid and robust films [7–9]. Although conducting polymers exhibit, in general, less electrical conductivity than metals, the conductivity as well as some other physical and chemical properties of such compounds, can be altered using dopants agents [10].

The theory of polaron and bipolaron can interpret the conductivity of conducting polymers. When polymers are oxidized or reduced, a polaron is formed, that is, the formation of a radical cation or radical anion is created, respectively. It is known as bipolaron when polarons are doble charged. Partial doping produces polarons, while doping at a higher level produces bipolarons. The formation of polarons and bipolarons, lows the energy gap ($E_g$) between the valence band (HOMO) and conduction band (LUMO) that results in the overlapping of the bands where the electrons are free to move in the conduction band thus, increasing the conductivity. The doping process increases the polymer's electrical conductivity by creating moving charges in the polymer structure [11,12]. Conducting polymers are semi-conductors in the neutral (non-doped) state, but in redox states the bandgap energy is reduced, and the electrical conductivity increases. For example, in the case of PPy, the bandgap energy is 3.16 eV in the neutral state, while the bandgap energy decreases to 1.72 eV in the fully doped state [13,14]. The doping process in polymers consists of adding electron donor or acceptor species to their molecular structure. The presence of dopants causes a significant change in the molecular structure of the polymer compared to the non-doped state [15]. Oxidation produces a polymer with a positive charge, which is known as p-doping. On the other hand, reduction produces a polymer with a negative charge, which is known as *n*-doping [16,17].

PPy and its derivatives are among the most well-known electroactive and conducting polymers. The oxidation potential for pyrrole (0.8 V) is lower than for other aromatic monomers; thus it is synthesized both chemically and electrochemically in a wide range of organic and aqueous solvents [18–21]. Indeed, PPy is one of the few conducting polymers that can be produced in aqueous solutions. Additionally, PPy has been considered more than other conducting polymers due to its high conductivity, ease, and flexibility in production, stability, and satisfactory mechanical properties [22,23]. Hence, PPy has various applications, such as in electronic and electrochromic systems [14,24–26], as capacitors [27,28], in sensors [29–32], in light batteries [33–35], and in separating membranes [36,37].

Although there are various methods for the synthesis of conducting polymers, electrochemical polymerization is preferable for various reason, such as easy control of the thickness, and high polymerization speed [38]. The use of dopants affects the general features and thermal stability of PPy [39–41]. The presence of dopant anions, which must be electrochemically stable, creates a charge balance in the polymer structure. The use of aqueous solutions in the synthesis of PPy significantly increases the selectivity of the dopants, which can be small or large compounds anions. The type, size, three-dimensional structure, charge, and electronic structure of the dopant, the deposition conditions, the electrode substrate, and solvent used determine the properties of PPy film produced by electrochemical synthesis [23,42–44]. Polyelectrolytes or anionic surfactants are examples of large dopant anions. Unlike small dopants, which enter and exit from the polymer matrix processes, large anions usually remain immobile and stable in the polymer structure. In the latter case, cations present in the electrolyte solution balance the charge during electrochemical processes (i.e., the penetration and escape of cations during the electrochemical reduction and oxidation of PPy, respectively). Moreover, PPy doped with polyanions is provided with stability and mechanical properties [41,45,46].

Very limited studies using dyes as dopants in PPy, have concluded that the electrochromic properties improved because of the conjugated properties of such compounds [47–52]. Moreover, investigations showed that dyes can also be placed between polymer chains, creating nano-pathways for better electron transfer. In addition, the previous study [53] showed that simultaneous use of dye molecule (AR18) and surfactant (SDS) as a dopant agent in polypyrrole had improved the electrochemical properties of the polypyrrole layer produced.

The present study aims to determine the effect of the molecular structural properties of the dye on the properties of PPy layers. Therefore, three dyes, which differ in the size and the number of negatively charged groups, have been used separately as dopants with SDS of PPy. The morphology and the electrochemical, optical, and electrochromic properties of the resulting PPy films have been investigated. It should be noted that the Acid Brilliant Scarlet 3R (AR18) and Amido Naphthol Red G (AR1) dyes (Fig. 1) have similar dimensions, but a different number of negatively charged groups. In contrast, AR1 and Indigo Carmine (IC) dyes have the same number of negatively charged groups, but different molecular sizes.

## 2. Experimental

### 2.1. Materials

Pyrrole (Py) from Aldrich was double distilled and kept in a refrigerator in a dark BG Bottle before use. Anhydrous lithium perchlorate ($LiClO_4$) of analytical reagent grade was used as the electrolyte and dopant for the control sample (Sigma-Aldrich). AR1 from Sigma-Aldrich, AR18 from Panreac, IC from Merck, and sodium dodecyl sulfate (SDS) from Sigma were used as dopants. All of the solutions were made using Milli-Q water.

### 2.2. Electropolymerization of doped PPy

Polypyrrole (PPy) films were electropolymerized on ITO-PET sheets using $ClO_4^-$ (control sample) AR1, AR18, IC, and SDS as dopant agent. In the case of the PPy/$ClO_4^-$ chronoamperometry was applied to a solution consisted of lithium perchloride and the pyrrole monomer and water. Whereas, the solutions prepared for obtaining PPy/IC-SDS films contained water, dye molecule (IC), surfactant (SDS), and pyrrole monomer. The PPy/dopant films were prepared on the conductive electrode (ITO-PET). by chronopotentiometry (CP), applying constant currents of 1.5 mA/cm$^2$ for PPy/$ClO_4^-$, and 1.0 mA/cm$^2$ for PPy/AR18, PPy/SDS, PPy/AR18-SDS, PPy/AR1-SDS, and PPy/IC-SDS for 150–200 s. After producing the films, an aqueous solution of lithium perchloride was used as an electrolyte to investigate their electrochemical and electrochromic behavior.

The volume of each synthesis solution was 10 mL, and the concentration of the materials in the aqueous synthesis solution used is shown in Table 1. All PPy films were synthesized using a three-electrode one-compartment cell at room temperature. After preparing the aqueous synthesis solutions with a certain amount of monomer (Py) and dopants, the oxygen was replaced by injecting nitrogen (99.995% in purity) for 10 min. ITO-PET sheets were used as a working electrode with 1 × 1.5 cm$^2$ area with 60 Ω/sq surface resistance, while stainless-steel sheets (AISI 316L) were used as a counter electrode with a surface of 1.5 × 2 cm$^2$. The Ag|AgCl electrode that contained a saturated KCl aqueous solution was used as a reference electrode.

The electropolymerization of PPy is affected by various parameters, including the electrochemical method used, the current or potential applied, the deposition duration, the concentration of each material, the dopant, and the type of solvent. These factors were optimized in a previous work [53]. In the present work, the optimal conditions were

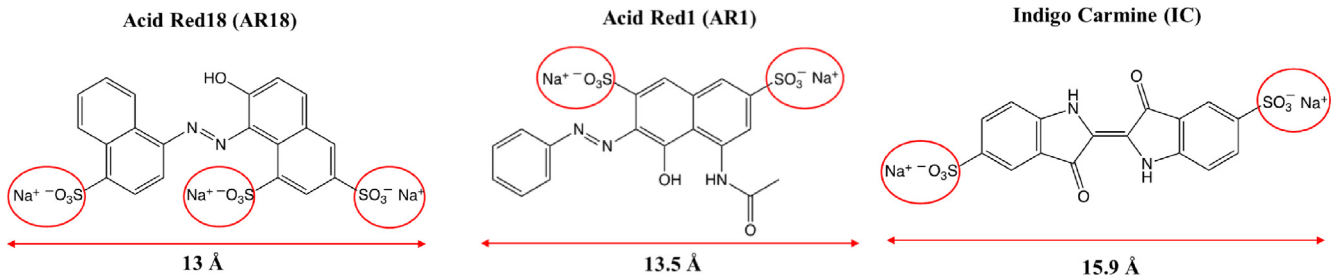


**Fig. 1.** Chemical structure of dye Acid Red1, Acid Red18, and Indigo Carmine. The size of molecules was measured with ChemDraw software.

**Table 1**
Concentration of dopants used for the electrodeposition of PPy films on the ITO-PET sheet. Electropolymerization of PPy was performed by CP at 1–1.5 mA/cm$^2$ for 150–200 s duration. The concentration of Py monomer was 0.1 M in all cases.

| PPy film | [$ClO_4^-$] (M) | [SDS] (M) | [AR18] (mM) | [AR1] (mM) | [IC] (mM) | Thickness (μm) |
|---|---|---|---|---|---|---|
| PPy/$ClO_4^-$ | 0.1 | – | – | – | | 5.0 ± 0.3 |
| PPy/SDS | – | 0.1 | – | – | | 5.0 ± 0.3 |
| PPy/AR18 | – | – | 0.5 | – | | 5.0 ± 0.2 |
| PPy/AR18-SDS | – | 0.1 | 0.5 | – | | 5.1 ± 0.2 |
| PPy/AR1-SDS | – | 0.1 | – | 0.5 | | 4.9 ± 0.2 |
| PPy/IC-SDS | – | 0.1 | – | – | 0.5 | 5.0 ± 0.2 |

used for all produced films. All PPy/dopant films have almost the same thickness and a good electrochemical response.

### 2.3. Equipment

Electrochemical analyses were performed using an Autolab PGSTAT302N potentiostat/galvanostat (Ecochimie, the Netherlands) and a conventional three-electrode system. Autolab devices were equipped with NOVA software and interfaced to the PC system. The range of potential was selected between − 1.0 V and + 1.0 V vs Ag|AgCl, using 0.1 M $LiClO_4$ aqueous solution as electrolyte. The scan rate was 100 mV/s in all cases.

Electrochromic parameters and absorption spectra of PPy layers were determined using in-situ spectroelectrochemical techniques. A VSP100 potentiostat model (EC-Lab V9.51 software) was coupled to an L12090 Hamamatsu spectrophotometer (Bio-Kine 32 V4.46 software). The electrodes used in the spectroelectrochemical studies included the PPy/dopant coating on ITO sheets as working electrode, a Pt wire counter electrode, and a saturated calomel electrode (SCE) as reference electrode. Finally, a 0.1 M $LiClO_4$ aqueous solution was used as the electrolyte in all measurements.

Surface morphology of films was evaluated using a Zeiss Neon 40 analytical field emission scanning electron microscope (FESEM). The applied voltage for observation was 5 kV. Energy dispersive X-ray (EDX) spectroscopy was performed with the same scanning electron microscope.

Topographical analyses of the films were conducted by atomic force microscopy (AFM) using a VEECO Dimension 3100 model, with a Molecular Imaging PicoSPM using a NanoScope IV controller under ambient conditions. The tapping mode AFM was operated at constant deflection. The row scanning frequency was set to 1 Hz. AFM measurements were performed on various parts of the layers, which provided reproducible images similar to those displayed in this work. The statistical application of the NanoScope Analysis software was used to determine the root mean square roughness ($R_q$), which is the average height deviation taken from the mean data plane.

A Dektak 150 stylus profilometer (Veeco, Plainview, NY, USA) measured the thickness of layers.

The optical characterization and the electrochromic performance of PPy/dopants films were recorded by *in situ* spectroelectrochemistry in the absorption mode.

## 3. Results and discussion

### 3.1. Electrochemical behavior

PPy/dopants films electrodeposited on ITO-PET sheets were washed with distilled water and dried in the vacuum oven at room temperature. The successful incorporation of the dyes was investigated by FTIR, Raman and energy-dispersive X-ray (EDX) spectroscopies and scanning electron microscopy (SEM). The most successful evidences were achieved by EDX, as is shown below in the morphological study. Unfortunately, the noise added by oxidized PPy, the charged sulfonyl groups, the sodium, and the low amount of dyes as dopant agents make difficult by FTIR and Raman spectroscopies. However, Raman spectra allowed to identify some shoulders that were attributed to the sulfonyl and azo groups of the dyes. This is illustrated in Fig. S1, which compares the spectra and micrographs recorded by μ-Raman for PPy/SDS, PPy/AR18-SDS and PPy/AR18. Despite the remarkable differences found in the superficial morphology, the spectra recorded for the three samples are very similar. However, the band at 1047 cm$^{-1}$ ($SO_3^-$) and the shoulders at 1454 cm$^{-1}$ (N═N) and 1534 cm$^{-1}$ (Azo-benzyl) suggest the incorporation of the dye.

The electrochemical behavior of the films was determined by cyclic voltammetry (CV), using a $LiClO_4$ 0.1 M aqueous solution as electrolyte. The voltammograms of all PPy/dopants, with exception of PPy/IC-SDS, were reported in a previous work [53]. Fig. 2 compares the voltammogram of PPy/IC-SDS with those recorded for PPy/AR18-SDS and PPy/AR1-SDS after 25 consecutive redox cycles. Since during successive cyclic in CV diagrams of each layer, the area between the oxidation and reduction curves is almost constant, so the doping of the dye molecule and the surfactant in the polymer chains is definite. Also, the comparison of CV diagrams of the layers showed that the electrochemical activity of PPy/AR18-SDS is higher than that of PPy/AR1-SDS and PPy/IC-SDS, which is probably due to the number of anionic groups and dimension of the dye. As the number

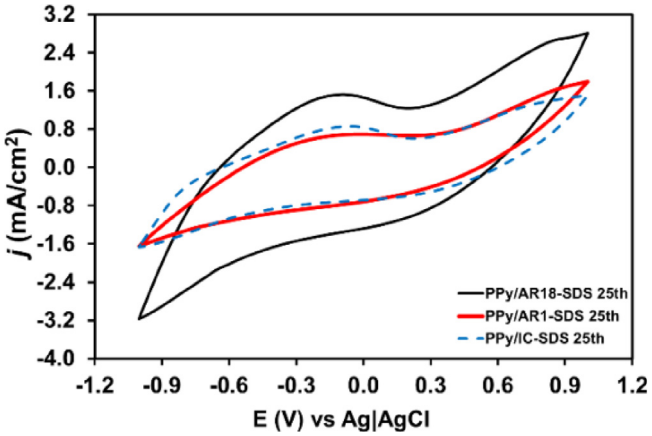


**Fig. 2.** Cyclic voltammograms for PPy/AR18-SDS, PPy/AR1-SDS, and PPy/IC-SDS layers after 25 redox cycles in 0.1 M $LiClO_4$ aqueous solution. Scan rate: 100 mV/s.

of anionic groups increases and the dimension of the dye decreases, the redox capacity of the PPy film increases, suggesting that the number of charge carriers in the polymer matrix increases with the negatively charged density groups. Also, the distance between the polymer chains decreases by reducing the size of the dye, enhancing the charge transfer rate, and the electrochemical activity. Therefore, the properties of the PPy/dopant film are affected by two factors: the number of negatively charged groups in the dopant, and its dimensions. According to Fig. 1, the AR18 has a smaller size in comparison to AR1 and IC. Besides, AR18 has three anionic groups, while AR1 and IC have only two. These results are while all the conditions of synthesis at each layer, including the method and the concentration of materials, are the same, just only the type of dye molecule is different between the PPy layers.

The diagrams of the current density of PPy/AR1-SDS and PPy/IC-SDS films and the voltammograms after 2 and 25 redox cycles are shown in Fig. 3. The presence of AR1 and IC dyes improves the electrochemical behavior of the PPy layers, with the electrostability increasing 14% and 10% for PPy/AR1-SDS and PPy/IC-SDS, respectively, after 25 consecutive redox cycles. This self-electrostabilizing behavior has been attributed to the presence of the dye, which facilitates the transfer of electrons among the polymer chains. The limit of current density in each redox cycle was higher for PPy/IC-SDS than for PPy/AR1-SDS, which has been associated to the larger size of IC.

### 3.2. Morphological and topographical characterization

Fig. 4 (left) shows representative scanning electron microscopy (SEM) images of PPy/SDS, PPy/AR18-SDS, PPy/AR18 and PPy/IC. Although all samples displayed a globular morphology, this is more compact for films without SDS. Thus, the size of the globules is higher for PPy/SDS and PPy/AR18-SDS than for PPy/IC and, especially, PPy/AR18. Energy dispersive X-ray (EDX) spectra, which are included in Fig. 4 (right), show the presence of sulfur and sodium, demonstrating the successful incorporation of the SDS and the dyes as dopant agents. Thus, the characteristic signal of sulfur, which comes from the sulfate of SDS and the sulfonate of dyes, is clearly detected in all spectra. Instead, the sodium signal is only observed for SDS-containing films. This has been attributed to the content of the different dopant agent, which in turn is related to the flexibility of SDS and the rigidity of AR18 and IC. Thus, the entrance of flexible SDS in the polymeric matrix is easier than that of rigid dyes and, therefore, the content of the former is expected to be higher than that of the latter. Accordingly,

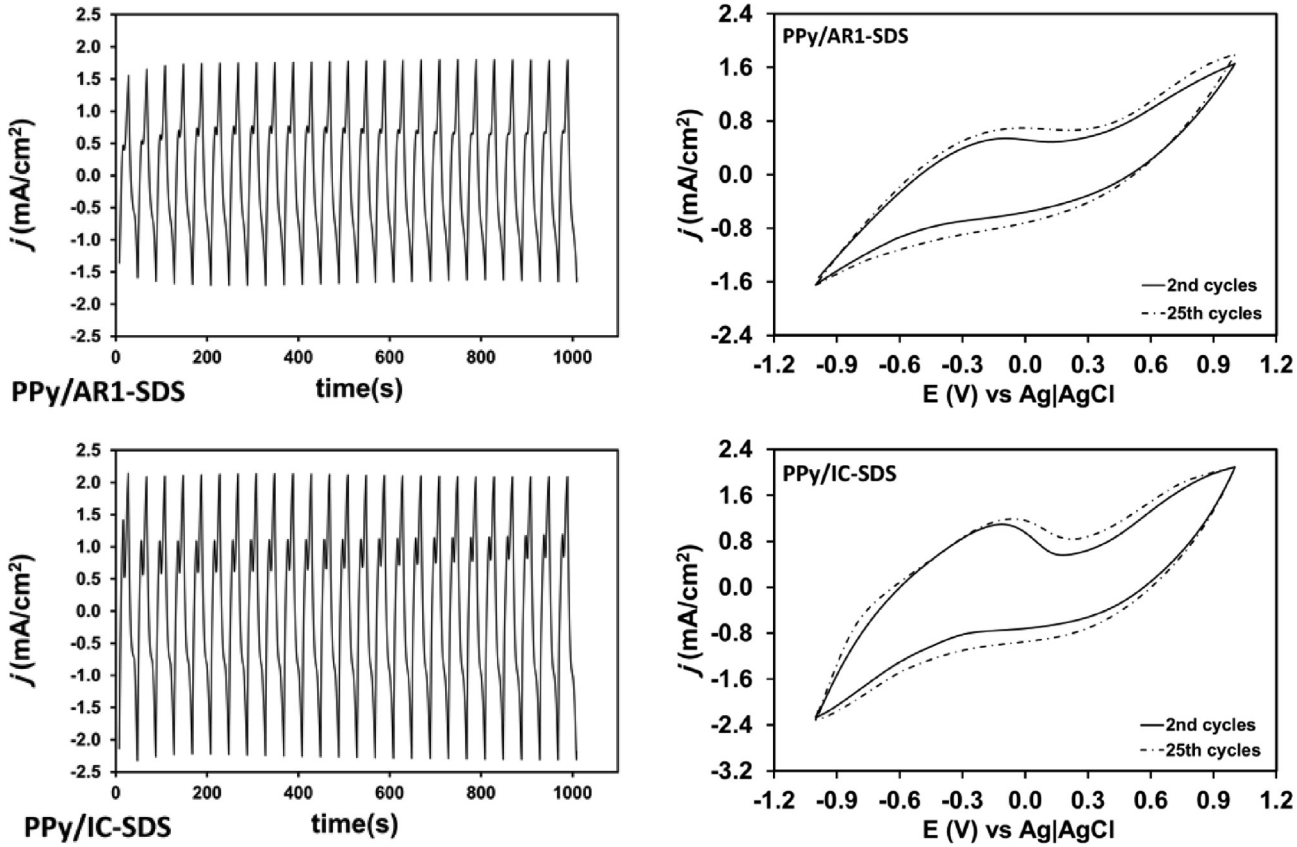


**Fig. 3.** Variation of the current density versus the time (left). Voltammograms for PPy/AR1-SDS and PPy/IC-SDS after 2 and 25 redox cycles (right).

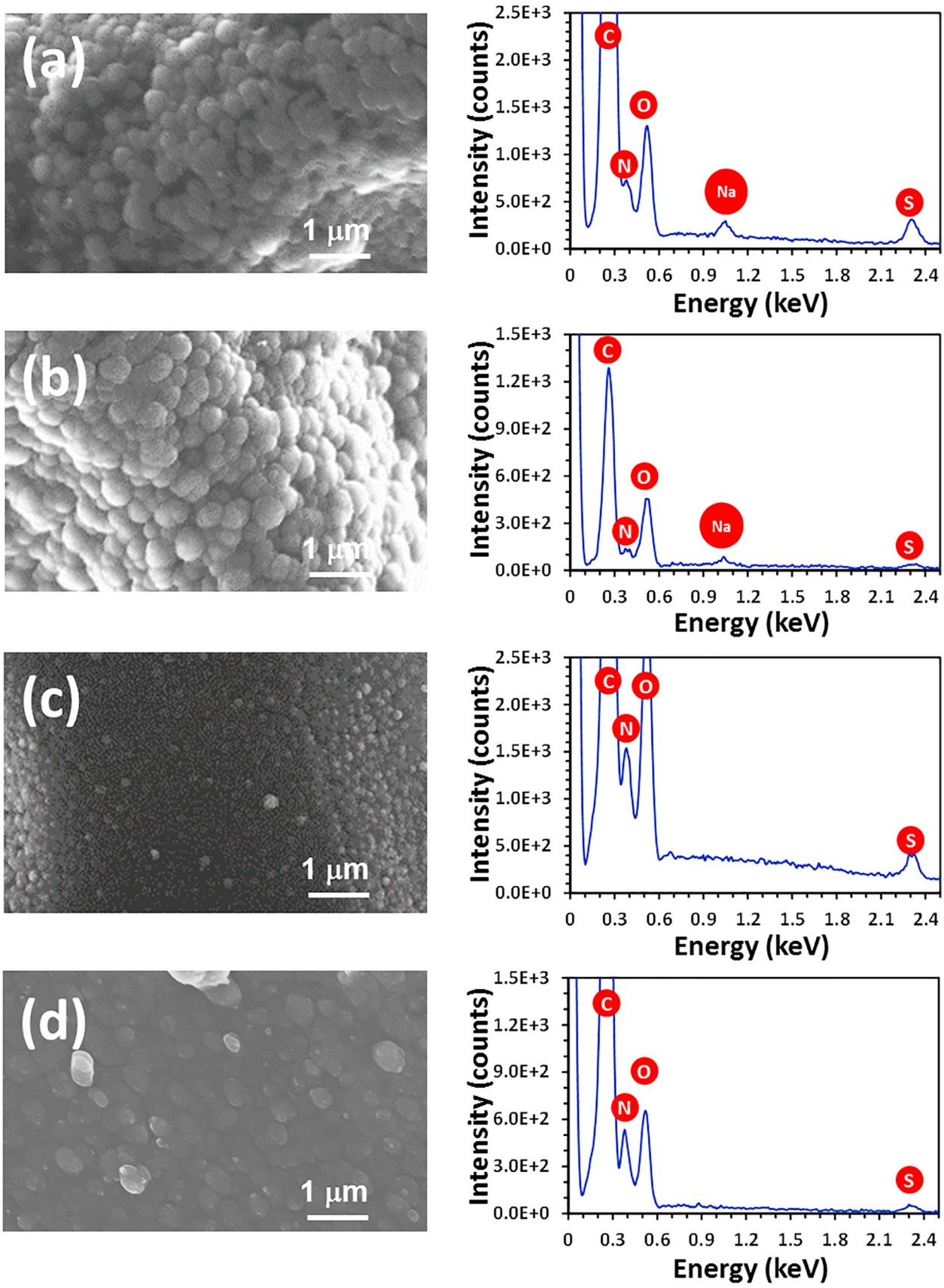


**Fig. 4.** Representative SEM micrograph (left) and EDX spectrum (right) of (a) PPy/SDS, (b) PPy/AR18-SDS, (c) PPy/AR18 and PPy/IC.

| | PPy/SDS | PPy/AR18 | PPy/AR18-SDS | PPy/AR1-SDS | PPy/IC-SDS |
|---|---|---|---|---|---|
| $R_q$ (nm) | 766 | 576 | 1434 | 1364 | 1030 |

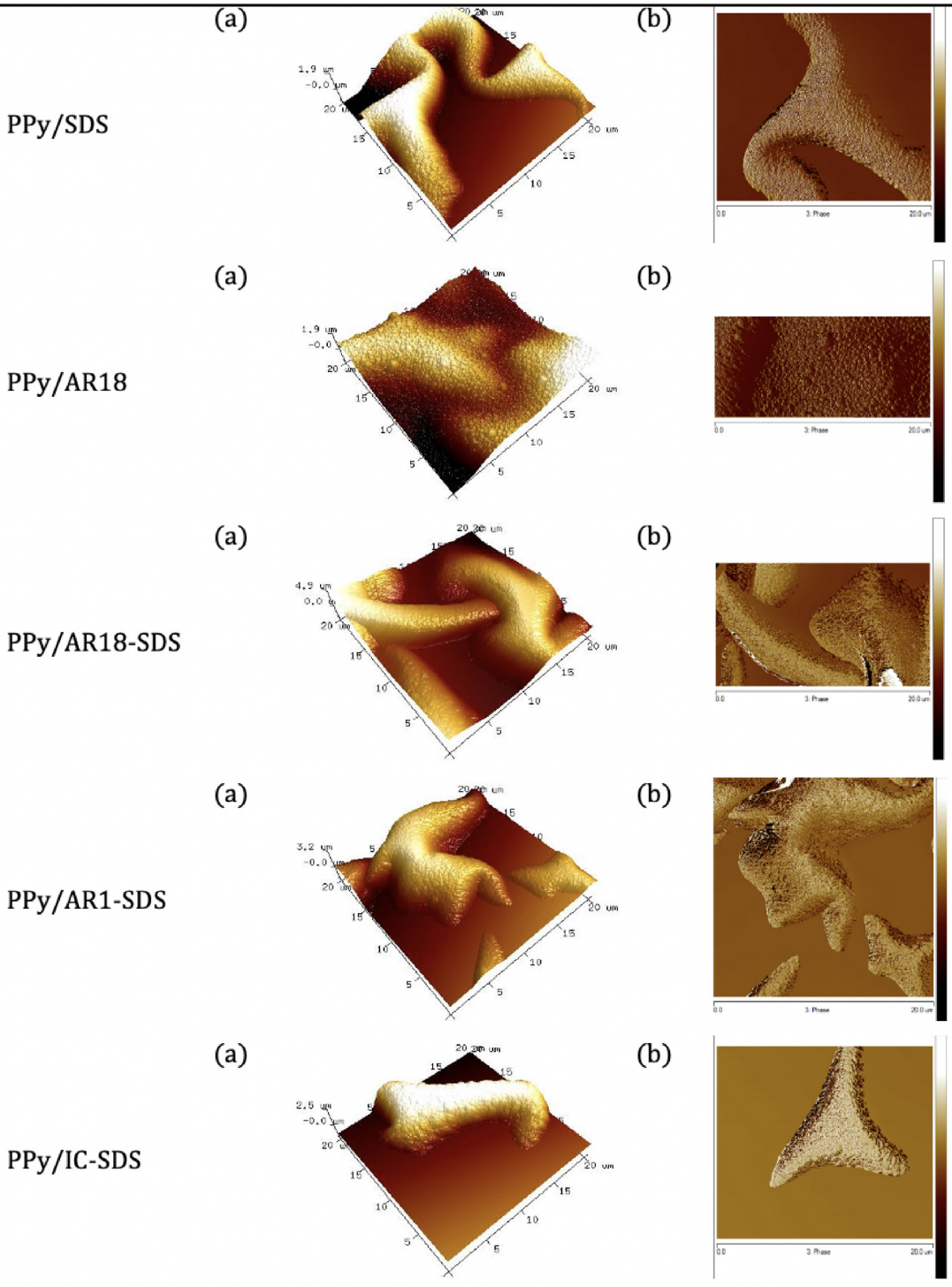


**Fig. 5.** The 3D (a) and 2D (b) AFM images for PPy/SDS, PPy/AR18, PPy/AR18-SDS, PPy/AR1-SDS, and PPy/IC-SDS films.

**Table 2**
Surface Roughness ($R_q$) for different PPy films. This data was measured with NanoScope Analysis software of AFM images.

| | PPy/SDS | PPy/AR18 | PPy/AR18-SDS | PPy/AR1-SDS | PPy/IC-SDS |
|---|---|---|---|---|---|
| $R_q$ (nm) | 766 | 576 | 1434 | 1364 | 1030 |

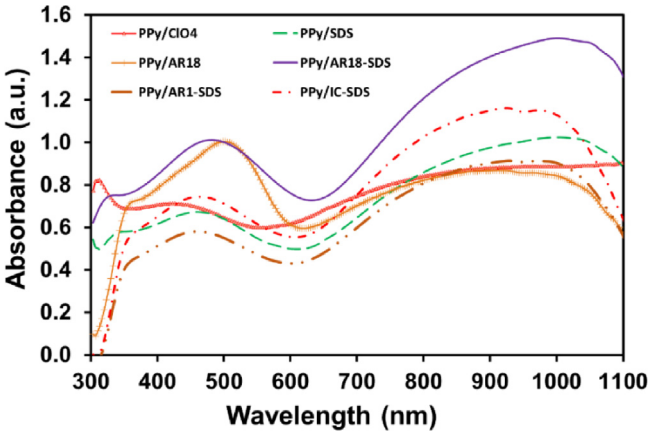


**Fig. 6.** UV–Vis-NIR spectra for PPy/$ClO_4^-$, PPy/SDS, PPy/AR18, PPy/AR18-SDS, PPy/AR1-SDS, and PPy/IC-SDS films.

**Table 3**
Energy bandgap ($\varepsilon_g$) and maximum absorption wavelength ($\lambda_{max}$) of PPy layers.

| System | $\lambda_{max}$ (nm) | $\varepsilon_g$ (eV) |
|---|---|---|
| PPy/$ClO_4^-$ | 426, 936 | 1.3 |
| PPy/AR1-SDS | 462, 930 | 1.37 |
| PPy/SDS | 462, 999 | 1.41 |
| PPy/IC-SDS | 462, 924 | 1.44 |
| PPy/AR18-SDS | 428, 1003 | 1.45 |
| PPy/AR18 | 502, 914 | 1.75 |

the sodium signal detected in PPy/SDS and PPy/AR18-SDS spectra corresponds to the sodium ions necessary for neutralizing the sulfate groups of exceeding SDS molecules.

The topographical characterization of the films was performed with AFM (Fig. 5), the surface roughness ($R_q$) being measured with NanoScope software (Table 2). Results indicate that the type of dopant affects the surface characteristics of the produced films. The presence of a surfactant as a dopant in PPy/SDS increases the $R_q$ compared to the presence of the dye molecule as a dopant in PPy/AR18, which may be related to the opening of the polymer structure in the presence of SDS. The combination of a dye and SDS in PPy/AR18-SDS has a synergistic effect on $R_q$, these results being consistent with those of Girotto and de Paoli [48]. The comparison of films with different dyes as a dopant shows that $R_q$ decreases with increased linear structure and amount of negatively charged groups: $R_q$ for PPy/IC-SDS < $R_q$ for PPy/AR1-SDS < $R_q$ for PPy/AR18-SDS.

### 3.3. Optical characterization

To investigate the optical behavior of the PPy/dopant films, absorption spectra were recorded in the UV–Vis-NIR wavelength range in natural states. As shown in Fig. 6, the absorption spectra changed with the presence of the different dopants. The optical bandgap energy of the PPy was calculated using Eq. (1) [53]:

$$\varepsilon_g = \frac{h \times c}{\lambda^{onset}} = \frac{1240}{\lambda^{onset}} \quad (1)$$

where $h$ is the Plank constant, c is the speed of light and $\lambda^{onset}$ is the collision point of the tangent line to the absorption spectra in $\pi - \pi^*$ transmissions.

The results, which are listed in Table 3 show two $\lambda_{max}$ for each film, confirm the formation of PPy. Thus, the absorption in the range of 400–500 nm is related to $\pi$-$\pi^*$ transfers in the neutral and polaron state, while absorption at $\lambda_{max} > 700$ nm is related to bipolaron mode in PPy chains [51].

The optical bandgap energy of PPy was 3.16 eV in the neutral state. This value decreases to 2.26, 1.76, and 1.46 eV for the polaron, bipolaron, and the fully doped state, respectively [14]. The values of $\varepsilon_g$ displayed in Table 3 indicate that PPy is in fully doped and bipolaron states in all films prepared in this work, no significant difference among the different PPy/dopants films being detected.

### 3.4. Spectroelectrochemical characterization

The spectroelectrochemical properties of PPy layers electrodeposited on transparent ITO-PET electrodes are studied using a 0.1 M aqueous solution of $LiClO_4$ as supporting electrolyte. A UV–Vis spectrometer, in the absorbance mode, is coupled and synchronized to a potentiostat and CVs with scan swept 0 V/ −1 V/ +1 V and 10 mV/s scan rate is carried out. Fig. 7 corresponds to the 3D and 2D absorption spectrum for each PPy layer and significant differences are found for each sample. In general, when the potential is shifted from − 1 V to + 1 V, the absorbance decreases at $\lambda_{max}$ 410 nm range while it increases in the range of 650–1100 nm. This spectroscopic response is likely to be due to a change in the PPy chains from the polaron form to the bipolaron one [51]. Therefore, the higher the number of bipolarons, the lower is the energy bond in the polymer, which resulted in the wavelength shift to larger values when oxidized, and the higher is the conductivity of the polymer (Fig. 6) [14].

The potential sweep of the voltametric measurement, at slow scan rate (10 mV/s), allowed determining that the intensity and width of the peaks were gradually changed at each small variation of potential. Moreover, the $\lambda_{max}$ and shape of each spectrum was different, indicating that the PPy layers have unique colors at each voltage. Thus, it is possible to have different colors in the PPy layers and achieve a multicolor electrochromic layer with different dopants in the PPy chains. Furthermore, the comparison of the PPy layers showed that the absorption intensity at $\lambda_{max}$ for thin films of 5 $\mu m$ thickness, in oxidized or reduced form, was high, so that the color change was recognizable to the naked-eye for all layers except the control layer (PPy/$ClO_4^-$). But as in Fig. 7, the absorption spectrum changed by applied voltage in each layer. This change in the absorption spectrum is mean creating a different color in the layer. To better understand these color changes, the color calculations were performed at − 1, 0, and 1 voltage. According to Table S1, the dopant type is very effective in the final color of the layer. Hence, in the next section, the electrochromic parameters were investigated in PPy/dopant for a better comparison of layers.

### 3.5. Electrochromic parameters

Several electrochromic parameters - color contrast, response time, coloration efficiency, and cyclability- that describe the spectroelectrochemical responses of prepared PPy films, are determined in this section, since the final applications of the PPy films, markedly rely on these electrochromic properties. Apart from the intrinsic properties

PPy/$ClO_4^-$

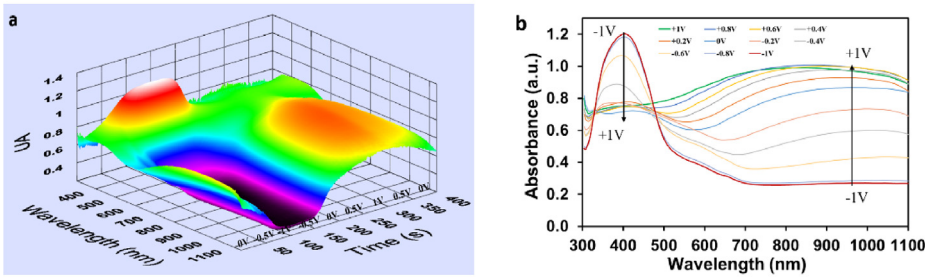


PPy/SDS

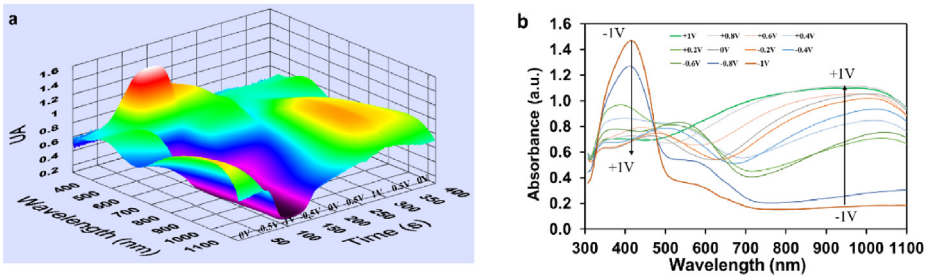


PPy/AR18

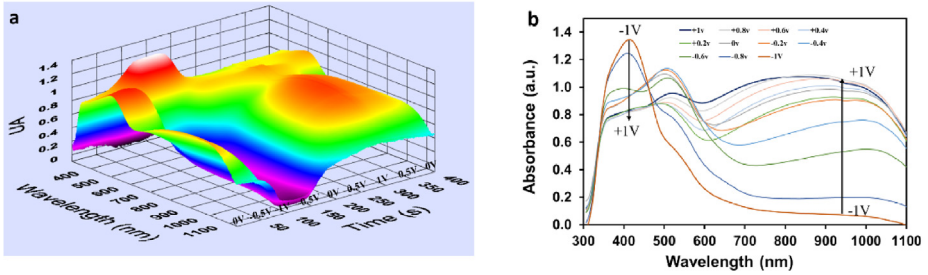


PPy/AR18-SDS

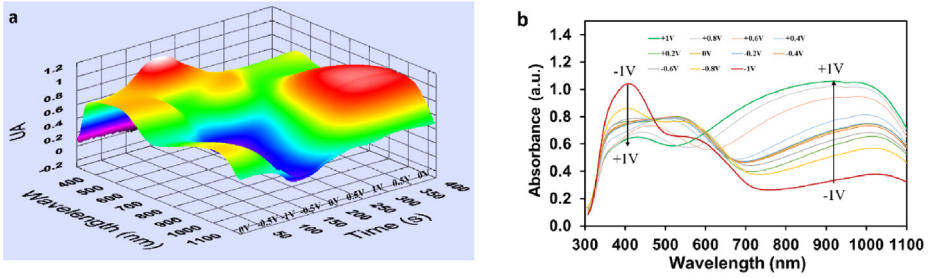


PPy/AR1-SDS

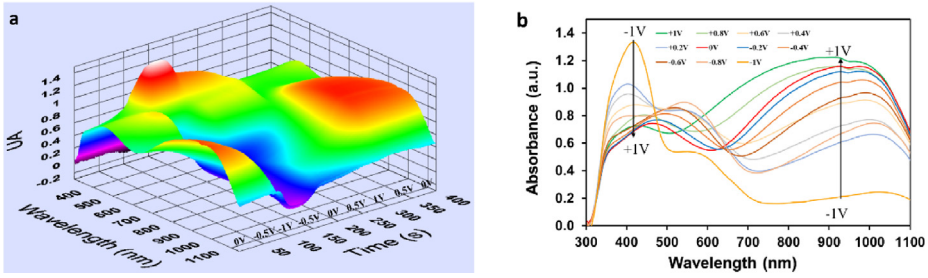


**Fig. 7.** Spectroelectrochemical behavior of PPy layers on ITO-PET sheets with different dopants in 0.1 M aqueous solution of $LiClO_4$ as supporting electrolyte during a 10 mV/s scan rate using CV in the scan sweep 0 V/ + 1 V/-1 V. The variation of absorption to wavelength to potential/ time in 3D (a) and 2D (b).

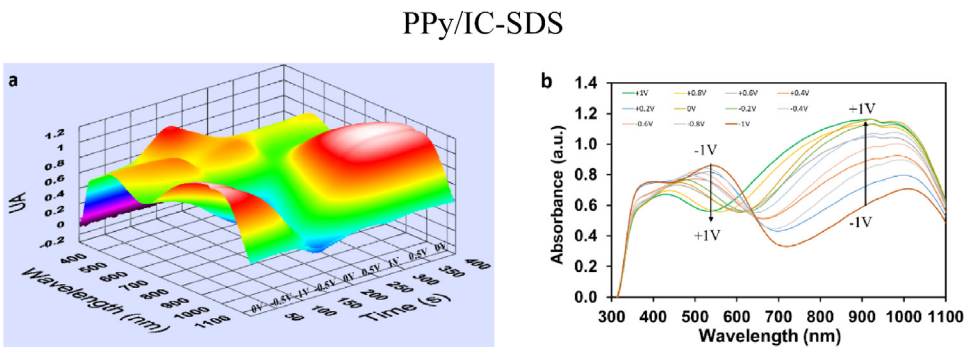


**Fig. 7** (*continued*)

of the electrochromic material (i.e., the PPy films), these parameters are strongly influenced by the ionic intercalation, necessary to compensate charges when the material is oxidized or reduced, since the amount and speed of electron and ion transfer between polymer chains, or interface between the polymer layer and electrolyte solution 36. For this reason, the use of stabilizers may help to enhance the ionic intercalation, and therefore the electrochromic performance.

In the present study, all the PPy films were synthesized using the CP method that allowed reproducible thicknesses and comparable films to be obtained. Ultimately, the electrochromic performance for each case can be compared in order to determine the effect of each additive in the final performance. For the spectroelectrochemical study, the chronoamperometric (CA) method was used to determine the electrochromic parameters for the PPy/dopants films (Fig. 8).

### 3.5.1. Color contrast

The color contrast is defined as the change in percentage of transmittance at $\lambda_{max}$ between the oxidized and reduced states of PPy ($\Delta T\% = T_{Reduced} - T_{Oxidized}$). The color contrast is influenced by the type of dopant, the synthesis conditions (such as temperature) that affect the ordination of the polymer chains, and the thickness of the polymer layer [14,50–52]. When the PPy coatings are very thin, the transmittance, which is proportional to the concentration of the species, is small, and therefore the color contrast as well. On the other hand, thicker layers are more opaque, and this makes it difficult to effectively change the color between the oxidized and reduced states [50]. This can be explained as the undoped form of PPy the neutral state- is an electrical insulator material [22]. To determine the color contrast at different wavelengths in the oxidized and reduced states (Table 4), [54] a constant potential of − 1 V is applied for 60 s followed by + 1 V for 60 s. The 2D and 3D spectra are shown in Fig. 8. The color contrast was determined at different wavelengths in the oxidized and reduced states (as shown in Table 4) [54]. Some of these wavelengths were: the wavelength of the maximum absorption spectrum in the neutral state of the polymer layers, the maximum wavelength in the oxidized or reduced states [54], the wavelength of $\pi - \pi^*$ transmission in polymer chains [55], and the wavelength in which the most significant absorption difference was observed between oxidized and reduced states [56]. Also, if the maximum variation of transmittance is higher than the visible wavelength range (>780 nm), it is referred to as the NIR optical contrast [57,58].

Therefore, in this study, the optical contrast of the produced layers is obtained at the $\lambda_{max}$ of the absorption spectrum in the oxidation and reduction states. Also, the optical contrast was obtained for all films at a constant wavelength in the visible region (Table 4).

The data in Table 4 show that the calculated color contrast is different depending on the $\lambda_{max}$, since the molar extinction coefficient, which measures how strongly a substance absorbs light, is characteristic at each wavelength. Therefore, the color contrast calculated at $\lambda_{max}^{Oxidized}$ (≈ 410 nm; yellow) of the PPy/dopant was higher than the $\lambda_{max}^{Reduced}$ (≈ 580–980 nm; dark green and blue), and the color contrast at a 780 nm wavelength was very close to the color contrast at $\lambda_{max}^{Oxidized}$.

In general, on comparing the electrosynthetized films PPy/dopant, they show enhanced color contrast with respect to the control sample (PPy/$ClO_4$) achieving an improvement of 29%. This result suggests that the type of dopants used, individually or simultaneously, has high positive effects on the properties of the PPy layers. In contrast to previous reports, the synthetized PPy/dopant films obtained in this study, show greater color contrast as shown in Table 5. Presumably, this fact is because of the suitability of the synthesis method and the proper placement of the dopants between the polymer chains, which eventually led to the high order of the polymer chains.

Studies of the dye molecule as dopant in PPy (PPy/AR18) increases the color contrast of the layers by 30%. According to Ferreira [50] and Tavoli [51], the reason for this improvement in the color contrast is because the dye molecule forms a nano-bridge between the PPy chains, which leads to an increase in the order of the PPy structure (as shown in XRD analysis). Ion and charge transfer in the PPy structures were improved due to the formation of the nano-bridge. The presence of large conjugated bonds in the dye molecule can also allow to establish electronic interaction with the π bonds of PPy chains, which can change the electronic properties of PPy. Finally, the presence of the dye molecule can keep the structure of PPy chains constant in the quinoid forms. This is associated with the formation of polaron and bipolaron in PPy chains, thus the color contrast of PPy layers was increased [49–51]. It is worthy to notice that the presence of three negatively charged groups in the case of AR18 instead of two sulfonate groups (IC and AR1) could help the formation of nano-bridges between PPy chains, therefore better color contrasts are obtained for the system PPy/AR18. Besides, the 41% of color contrast can be related to the stabilization of the reduced and oxidized form for the system PPy/SDS since SDS is a well-known stabilizing agent.

A comparison of the color contrast of the layers (for example, at 780 nm) showed that the simultaneous use of the dye molecule and the surfactant as a dopant (PPy/AR18-SDS layers) produces a higher color contrast than the separate use of the dopants for the electrochromic films. This increase confirms the synergistic effect of the dye molecule and the surfactant and also the effect of one does not interfere with the mechanism of the second. The comparison of the color contrast obtained for the three films PPy/AR18-SDS, PPy/IC-SDS, and PPy/AR1-SDS showed that the presence of AR18 dye molecule in the PPy structure had a better effect on the color contrast of the film. The AR18 dye molecule had 22% and 71% more color contrast than the layers containing the IC and AR1 Dye, respectively. The difference in the color contrast of the layers is likely to be related to the configuration of the dye molecule (i.e., the dimensions, the number of anion groups, and how the anion groups were placed in the dye structure). Each of these factors affects the placement of the dye molecule, the mode of electron transmission, and the amount of electron transfer between the polymer chains.

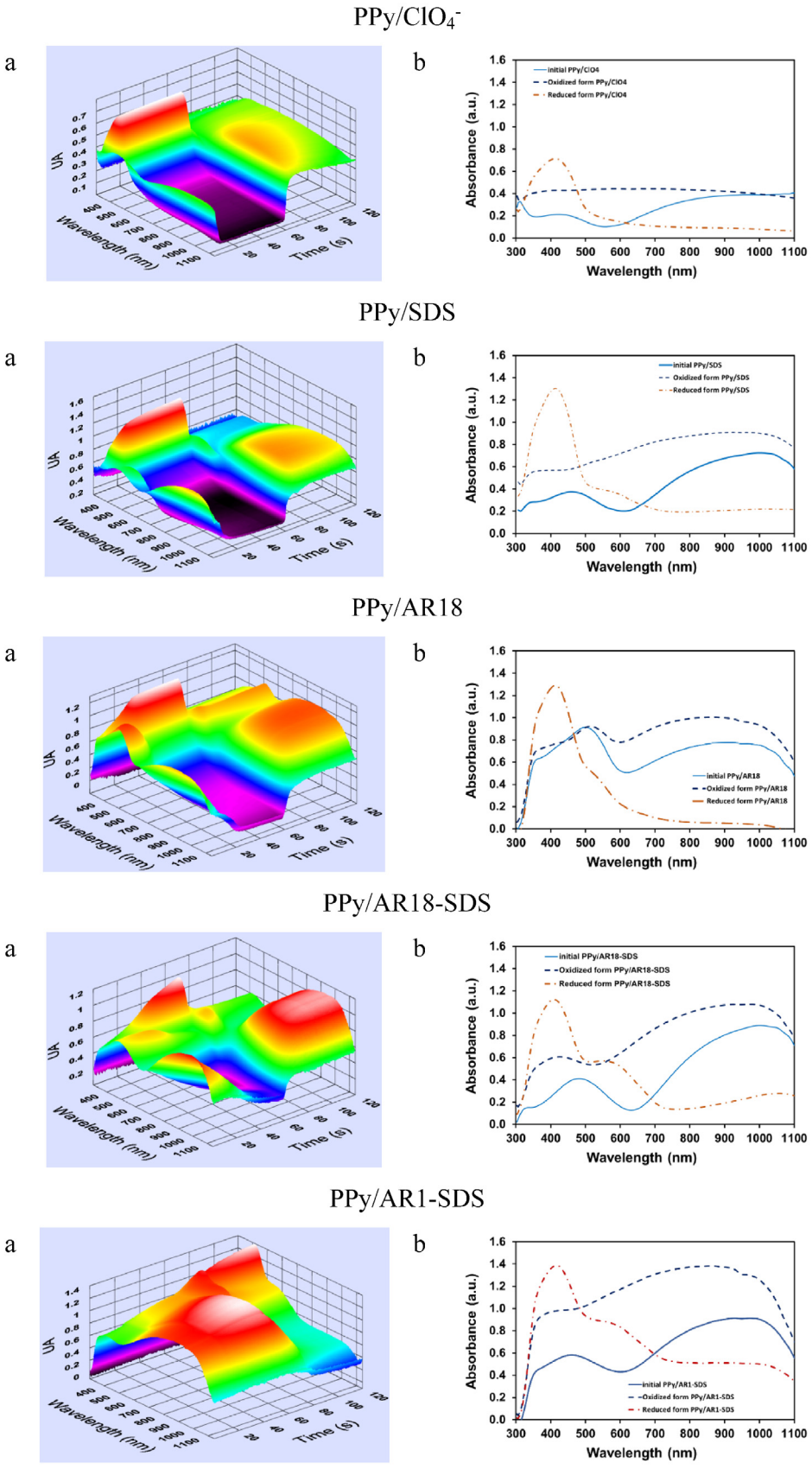


**Fig. 8.** Spectroelectrochemical behavior of PPy layers on ITO-PET electrodes with different dopants in 0.1 M $LiClO_4$ aqueous solution as supporting electrolyte. (a) 3D and (b) 2D spectrum for the samples when a constant potential of − 1.0 V vs SCE for 60 s is applied to obtain the reduced state (red dashed line) and + 1.0 V for next 60 s for the oxidized state (blue dashed line).

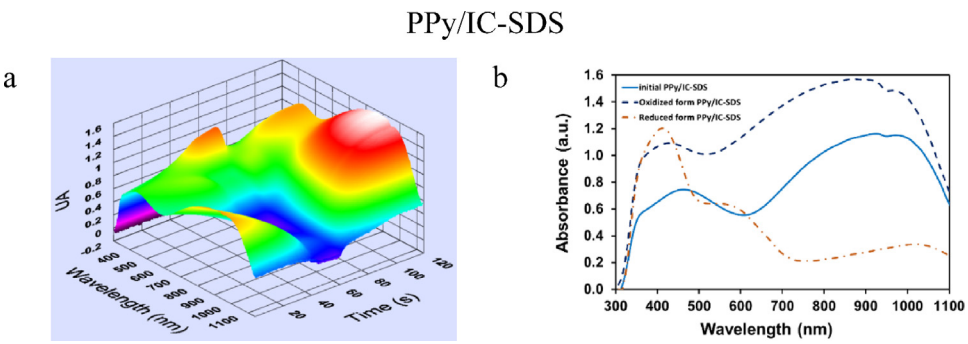


**Fig. 8** (*continued*)

**Table 4**
Color contrast for PPy layers at various wavelengths.

| System | $\lambda_{max}^{Reduced}$ (nm) | $\lambda_{max}^{Oxidized}$ (nm) | $\Delta T\%at\lambda_{max}^{Reduced}$ | $\Delta T\%at\lambda_{max}^{Oxidized}$ | $\Delta T\%at\lambda_{780nm}$ |
|---|---|---|---|---|---|
| PPy/$ClO_4^-$ | 412 | 581 | 16 | 21 | 26 |
| PPy/SDS | 413 | 927 | 29 | 41 | 41 |
| PPy/AR18 | 413 | 864 | 11 | 54 | 53 |
| PPy/AR18-SDS | 409 | 976 | 25 | 50 | 55 |
| PPy/IC-SDS | 413 | 871 | 14 | 44 | 45 |
| PPy/AR1-SDS | 419 | 861 | 13 | 33 | 23 |

**Table 5**
Comparison of color contrast and response time of different studies that used Dye.

| System | ΔT% | $\tau_c$(s) | $\tau_a$(s) | references |
|---|---|---|---|---|
| PPy-DS-IC | 37 (700) | 8 | | [48,49] |
| PPy/DS | – | 50 | | [49] |
| PPy-RB | 41 (795) | 14 | | [50] |
| PPy-DR | 23 (795) | 9 | | [50] |
| PPy-ECR | 27 (800) | <1.5 | | [52] |
| PPy-$ClO_4^-$ | 7 (800) | > 2 | | [51] |
| PPy-IC | 35 (700) | 12 | 3 | [52] |
| | 15 (530) | | | [52] |
| PPy-IC-$Au_{(nanoparticles)}$ | 44 (700) | 10 | 4 | [52] |
| | 22 (530) | | | [52] |

### 3.5.2. Response time

The response time is defined as the time required to change 90% of the transmittance of an electrochromic substance at a specific $\lambda$ [56–61]. For the response time calculations, CA measurements are performed by applying − 1.0 V, and a subsequent + 1.0 V vs SCE for 60 s. Note that the response time was usually measured between the coloring and bleaching states. However, in this study, coloring was seen in both oxidized and reduced states. Therefore, the response time of the electrochromic layer is different at each redox state, thus in this paper, two response times were defined; an anodic response time ($\tau_a$) and a cathodic response time ($\tau_c$) In order to facilitate the calculation of the response times, a part of the respective $\lambda_{Oxidized}^{max}$ and $\lambda_{Reduced}^{max}$ shown in Table 4 for each sample, two more $\lambda$ were fixed at 780 nm and 410 nm.

The results of the response times in the four wavelengths are shown in Table 6, whereas the response time diagrams for all PPy/dopants at $\lambda$ = 780 nm and $\lambda$ = 410 nm, are shown in Fig. 9. Note that the response times were shorter at $\lambda_{Oxidized}^{max}$ or $\lambda_{Reduction}^{max}$ for each sample with respect to the ones calculated at 780 and 410 nm. Furthermore, the anodic response times in PPy layers are more concise than the cathodic response times, which means that the cationic state of the doped PPy is more stable than their anionic state because of the $SO_3^-$ groups present in the structure. The data obtained for the response time of PPy layers showed that the type of dopants have an effect on the response time. In general, the smaller the size of dopant (for example, in PPy/$ClO_4^-$-layer), the shorter the response time of the layer, because the path of electrons is shorter, with response times below 60 s being obtained for all the samples. The presence of the dye molecule as a dopant (PPy/AR18) increased the response time compared to the use of the SDS surfactant as a dopant (PPy/SDS), due to the presence of conjugated bonds in the dye molecule structures. For the samples containing the dye and surfactant molecules (PPy/AR18-SDS) a slow response, in the order of seconds, is determined. Finally, a comparison between the response times of PPy films containing AR18, AR1, and IC molecules, shows that the fastest time response is obtained for PPy/AR18 because the dye molecule has more anion groups.

**Table 6**
Anodic and cathodic response times for electrochromic layers at a different wavelength.

| System | $\tau_c(s)at\lambda_{max}^{Reduced}$ | $\tau_a(s)at\lambda_{max}^{Oxidized}$ | $\tau_c(s)at\lambda_{410nm}$ | $\tau_a(s)at\lambda_{780nm}$ |
|---|---|---|---|---|
| PPy/$ClO_4^-$ | 3.8 | 6 | 3.8 | 3 |
| PPy/SDS | 12.9 | 7.5 | 12.5 | 9.2 |
| PPy/AR18 | 21.5 | 12.1 | 21.8 | 15 |
| PPy/AR18-SDS | 47.8 | 17.2 | 47.8 | 20.2 |
| PPy/IC-SDS | 48.5 | 29.8 | 48 | 31.3 |
| PPy/AR1-SDS | 45 | 21.9 | 44.9 | 22.5 |

In addition, it is known that the length of AR18 molecule is 13 Å, being smaller than the AR1 or IC, 13.3 Å and 15 Å, respectively. There seems to be a correlation between the response time and the dopant size, since, in the case of PPy/AR1-SDS, the response time is shorter than PPy/IC-SDS layers. Therefore, these results indicate that two factors affect the response time; the number of anion groups and the aspect ratio of the dopants structure. According to Fig. 1, the AR18 structure has both factors; hence PPy/AR18-SDS has a shorter response time compared to PPy/AR1-SDS or PPy/IC-SDS. If the number of anion groups is the same in different dopants, the dimensions of the dopant structure increase their influence on the properties. In the case of the two dyes, AR1 and IC, it was observed that PPy/IC-SDS exhibits a longer response time than PPy/AR1-SDS. Thus, the dimension of the structure determines the length of electron passages between the PPy chains.

However, the main improvement of the current synthesis methodology presented in this work does not rely on the enhancement of the response times, since, as shown in Tables 5 and 6, slower response times were obtained.

### 3.5.3. Coloration efficiency

The coloration efficiency ($\eta$) is defined as the change in the optical density (ΔOD) per unit of electric charge applied ($Q_d$) to the electrochromic material (Equation (2)). The ΔOD is calculated with the

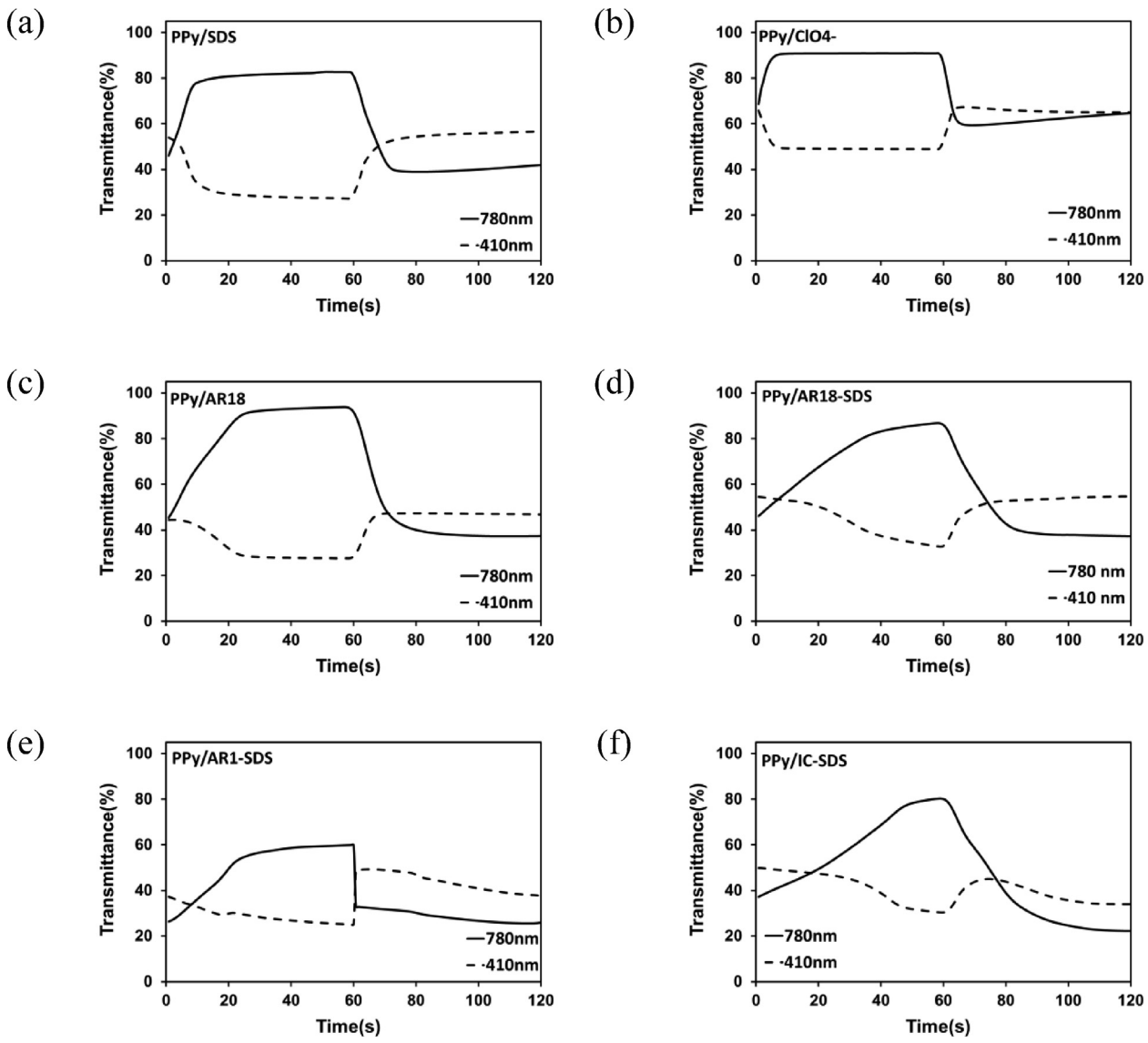


**Fig. 9.** The anodic (at 780 nm) and cathodic (at 410 nm) response time diagrams for (a) PPy/$ClO_4$, (b) PPy/SDS, (c) PPy/AR18, (d) PPy/AR18-SDS, (e) PPy/AR1-SDS, and (f) PPy/IC-SDS layers at same wavelength in the visible range.

**Table 7**
Coloration Efficiency of PPy / dopant films produced.

| System | $T_c/T_a$ at $\lambda_{max}^{Reduced}$ | $T_c/T_a$ at $\lambda_{max}^{Oxidized}$ | $T_c/T_a$ at $\lambda_{780nm}$ | $Q_c$ (mC) | $Q_a$ (mC) | $\eta_c$($cm^2$/C) | $\eta_c$($cm^2$/C) |
|---|---|---|---|---|---|---|---|
| PPy/$ClO_4^-$ | 0.75 | 1.33 | 1.4 | 20 | 34 | 70 | 41.2 |
| PPy/SDS | 0.52 | 2.68 | 2.5 | 27 | 50 | 277.8 | 150 |
| PPy/AR18 | 0.77 | 2.48 | 2.41 | 27 | 61 | 267.8 | 118.5 |
| PPy/AR18-SDS | 0.60 | 2.34 | 2.35 | 18 | 28 | 391.7 | 251.8 |
| PPy/IC-SDS | 0.73 | 2.18 | 2.18 | 39 | 23 | 167.7 | 284.4 |
| PPy/AR1-SDS | 0.74 | 1.9 | 1.86 | 24 | 35 | 323.5 | 159.4 |

ratio of the logarithm of $T_c$ % (transmittance of the reduced state) and $T_a$% (transmittance of the oxidized state) at $\lambda_{max}$ [14]. Hence, in our case the transmittance values are measured at $\lambda_{max}^{Reduced}$, $\lambda_{max}^{Oxidized}$, and 780 nm (Table 7) for PPy films with and without dopants, with the Tc/Ta at $\lambda_{max}^{Oxidized}$,ratio being very close to one in all the cases.

$$\eta = \frac{\Delta OD}{Q_d} = \frac{\log [T_c/T_a]}{Q/A} \quad (2)$$

The electrodeposition synthesis is fully controlled and optimized, all the resulting PPy films are 3 $cm^2$ of surface area. Table 7 shows the total charge required for the oxidation or reduction. In these studies, CA measurements are carried out by applying − 1.0 V and + 1.0 V vs SCE for 60 s each. This time was stipulated as that necessary to ensure the fully oxidized or reduced state of the polymer and thus obtain more accurate results. PPy is an electrochromic material in both

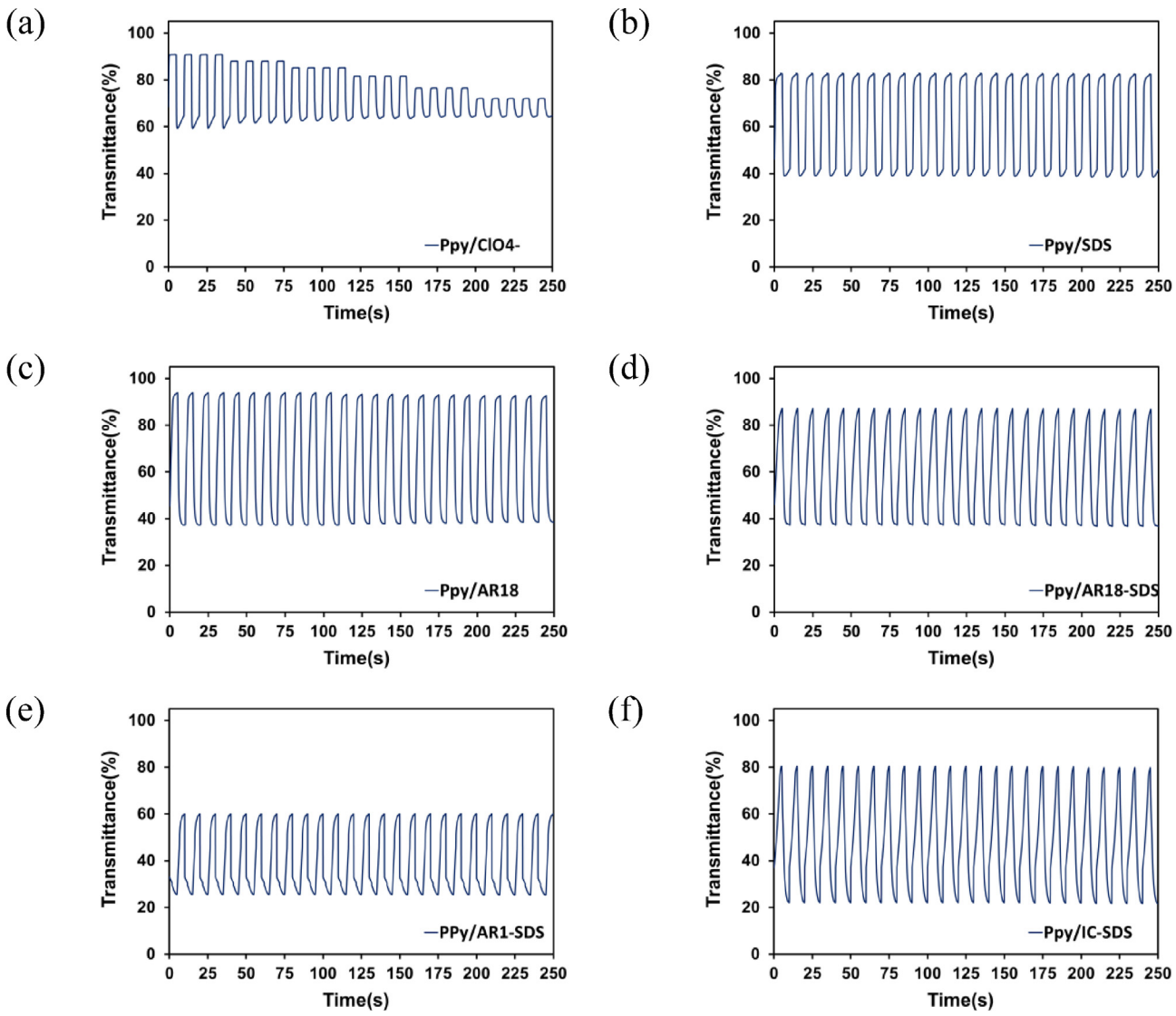


**Fig. 10.** Optical stability for (a) PPy/$ClO_4^-$,(b) PPy/SDS, (c) PPy/AR18, (d) PPy/AR18-SDS, (e) PPy/AR1-SDS, and (f) PPy/IC-SDS layers for oxidation (-1 V) and reduction (+1 V) state with 5 s residence time.

**Table 8**
Comparison of the color contrast of PPy films after 25 cycles.

| System | $\Delta T\%_{1ndcycle}$ | $\Delta T\%_{25thcycle}$ |
|---|---|---|
| PPy/$ClO_4^-$ | 26 | 5 |
| PPy/SDS | 41 | 41 |
| PPy/AR18 | 53 | 52 |
| PPy/AR18-SDS | 55 | 55 |
| PPy/IC-SDS | 45 | 45 |
| PPy/AR1-SDS | 23 | 23 |

the oxidation and reduction states, thus the cathodic coloration efficiency ($\eta_c$) and anodic coloration efficiency ($\eta_a$) are presented in Table 7.

As shown in Table 7, the use of large anions (surfactants and dyes) as dopants in the PPy layer has a more significant effect on the coloration efficiency of the electrochromic layers compared to small anions. In addition, the simultaneous use of the dye molecule and the surfactant had a beneficial synergistic effect on the coloration efficiency. This positive effect was observed in all the three dyes, especially the AR18 molecule in both $\eta c$ and $\eta a$. The reasons for this positive effect could be due to the opening of the PPy structure, as a result of the presence of the surfactant, which helps the dye molecule enter between PPy chains. Therefore, the participation of the dye in the conjugate system of the PPy increases the coloration efficiency of the PPy films. Another possible reason for the increase in the coloration efficiency when the dye and the surfactant are simultaneously used, is because of an increase in the charge of the PPy structure. Subsequently, the electron transport along the conjugated system is favored, and facilitates the color change when an electric potential is applied, since less total charge is needed in both the cathodic and anodic process. It is worth noting, that while there are slight differences in the Tc/Ta ratio between PPy layers, there is a noticeable difference in coloration efficiency. According to Equation (2), the coloration efficiency depends on $Q_d$, so as shown in Table 7, the $Q_a$ is greater than $Q_c$ for cases other than PPy/IC-SDS.

As a result, the coloration efficiency is different for each PPy/-dopant for both, $\eta c$ and $\eta a$, and in general ηc is higher than ηa in all electrochromic films except in case of PPy/IC-SDS film. Presumably, higher $\eta c$ values, compared to $\eta a$, are obtained because of the higher order of the polymer chains in the reduced state (i.e., PPy and dopants exhibit intermolecular interaction with π bonds that favors the rearrangement).

The PPy/AR18-SDS layer had a higher cathodic and anodic coloration efficiency than other layers, which is likely to be due to the presence of more anionic groups and smaller molecule dimensions in AR18. With these results, it has been demonstrated that several factors influence the electrochromic performance of PPy films, and the appropriate selection of dopants plays an important role (e.g., number of anion groups, the distribution of anion groups in the dopant structure, the dimensions of the dopant structure, and the existence of conjugated bonds) in order to enhance the coloration efficiency.

*3.5.4. Fatigue resistance*

The ability of the electrochromic material to undergo, and be stable, upon consecutive switching potentials, is known as electrochromic fatigue resistance [53]. For this study, cycles of − 1.0 V (5 s) and + 1.0 V (5 s) vs SCE are applied and repeated 25 times this is shown in Fig. 10. The color contrast of the films after 25 cycles indicates that all the electrochromic layers exhibit excellent optical stability, except the PPy/$ClO_4^-$ film (Table 8). Therefore, the use of SDS and dyes as dopants in the PPy electrosynthesis clearly has an effect on improving the fatigue resistance and thus the optical stability. In general, the results show that there is a close relationship between the electrochemical stability and optical stability; hence the samples that exhibit good electrochemical stability also have convenient optical stability.

## 4. Conclusions

In this study, PPy electrochromic films were produced using different dopant agents, such as surfactants (SDS), and three different Dyes (AR18, AR1, and IC). The results showed that the use of a Dye helps to improve the electrochemical behavior, optical characterization, and electrochromic properties of PPy layers, due to the presence of conjugated bonds. The simultaneous use of a Dye and SDS as a dopant showed a synergistic effect on the electrochemical stability of the films. Furthermore, the morphology of the PPy/dopants showed that the presence of a Dye with a linear structure reduced the surface roughness. Finally, it was observed that the presence of a Dye and SDS as a dopant reduced the optical bandgap energy of PPy and fully doped at PPy, which showed the positive effect of the dopants used and the excellent position of the dopant between the polymer chains.

The spectroelectrochemical behavior of layers showed that the absorption spectrum was exclusive for each film. Moreover, the type and size of the Dyes molecule structure, and the concentration of anions and their distribution had significant effects on the electrochromic properties of the films. The movement of electrons can be ameliorated by increasing the anion groups and reducing the size of the Dye' structures, since the charge was increased by the polymer structure, thus the color contrast and coloration efficiency of the electrochromic layers was improved. Moreover, the response time of electrochromic layers increased with longer dimensions of the Dye. Finally, a direct relationship was also observed between the electrochemical and electrochromic stability of PPy doped SDS and the Dye.

## CRediT authorship contribution statement

**Maryam Bayat:** conceptualization, investigation, methodology, formal analysis, Writing - original. **Dariush Semnani:** conceptualization, Writing - review & editing. **Mohammad Dinari:** conceptualization, Writing - review & editing. **Sara Santiago:** investigation, methodology, formal analysis, Writing - original draft. **Francesc Estrany:** conceptualization, methodoly, Writing - review & editing. **Hossein Izadan:** conceptualization, supervision, Writing - review & editing. **Carlos Alemán:** conceptualization, investigation, methodology, supervision, funding, Visualization, Writing - original draft, Writing - review & editing. **Gonzalo Guirado:** conceptualization, investigation, methodology, supervision, funding, Visualization, Writing - original draft, Writing - review & editing.

## Declaration of Competing Interest

The authors declare that they have no known competing financial interests or personal relationships that could have appeared to influence the work reported in this paper.

## Acknowledgements

The authors thank the Iran Ministry of Science, Research, and Technology for monetary support for the performance of this work at UPC, Spain during a research visit. The authors acknowledge MINECO/FEDER (RTI2018-098951-B-I00, CTQ2015-65439-R and PID2019-106171RB-I00) and the *Agència de Gestió d'Ajuts Universitaris i de Recerca* (2017SGR359). Support for the research of C.A. was received through the prize, "ICREA Academia" for excellence in research, funded by the *Generalitat de Catalunya*.

## Appendix A. Supplementary data

Supplementary data to this article can be found online at https://doi.org/10.1016/j.jelechem.2021.115113.

## References

[1] R.J. Mortimer, D.R. Rosseinsky, P.M.S. Monk, Electrochromic Materials and Devices, 1st ed., WILEY-VCH, Weinheim, Germany, 2005.
[2] J.R. Platt, Electrochromism, a possible change of color producible in dyes by an electric field, J. Chem. Phys. 34 (3) (1961) 862–863, https://doi.org/10.1063/1.1731686.
[3] P. Bamfield, Chromic Phenomena: Technological Applications of Colour Chemistry, 2nd ed., Royal Society of Chemistry, Cambridge, 2010. https://doi.org/10.1039/9781849731034.
[4] A.S. Ribeiro, R.J. Mortimer, Electrochromic polymers, in: Encycl. Polym. Sci. Technol., Wiley, 2015, pp. 1–27. https://doi.org/10.1002/0471440264.pst494.pub2.
[5] P.M. Beaujuge, J.R. Reynolds, Color control in π-conjugated organic polymers for use in electrochromic devices, Chem. Rev. 110 (1) (2010) 268–320, https://doi.org/10.1021/cr900129a.
[6] F. Bekkar, F. Bettahar, I. Moreno, R. Meghabar, M. Hamadouche, E. Hernáez, J.L. Vilas-Vilela, L. Ruiz-Rubio, Polycarbazole and its derivatives: synthesis and applications. A review of the last 10 years, Polymers (Basel) 12 (2020) 2227, https://doi.org/10.3390/polym12102227.
[7] T.-G. Sun, Z.-J. Li, J.-Y. Shao, Y.-W. Zhong, Electrochromism in electropolymerized films of pyrene-triphenylamine derivatives, Polymers (Basel) 11 (2019) 73, https://doi.org/10.3390/polym11010073.
[8] L. Beverina, G.A. Pagani, M. Sassi, Multichromophoric electrochromic polymers: colour tuning of conjugated polymers through the side chain functionalization approach, Chem. Commun. 50 (41) (2014) 5413–5430, https://doi.org/10.1039/C4CC00163J.
[9] M. Lahav, M.E. van der Boom, Polypyridyl metallo-organic assemblies for electrochromic applications, Adv. Mater. 30 (41) (2018) 1706641, https://doi.org/10.1002/adma.v30.4110.1002/adma.201706641.
[10] H.S. Nalwa, Handbook of Advanced Electronic and Photonic Materials and Devices, Ten-Volume Set, Academic Press, 2000.
[11] T. Nezakati, A. Seifalian, A. Tan, A.M. Seifalian, Conductive polymers: opportunities and challenges in biomedical applications, Chem. Rev. 118 (14) (2018) 6766–6843, https://doi.org/10.1021/acs.chemrev.6b00275.
[12] T.-H. Le, Y. Kim, H. Yoon, Electrical and electrochemical properties of conducting polymers, Polymers (Basel) 9 (2017) 150, https://doi.org/10.3390/polym9040150.
[13] M. Wan, Conducting Polymers with Micro or Nanometer Structure, Springer Berlin Heidelberg, Berlin, Heidelberg, 2008. https://doi.org/10.1007/978-3-540-69323-9.
[14] P. Camurlu, Polypyrrole derivatives for electrochromic applications, RSC Adv. 4 (99) (2014) 55832–55845, https://doi.org/10.1039/C4RA11827H.
[15] J. Heinze, B.A. Frontana-Uribe, S. Ludwigs, Electrochemistry of conducting polymers—persistent models and new concepts, Chem. Rev. 110 (2010) 4724–4771. https://doi.org/10.1021/cr900226k.
[16] H. Naarmann, Polymers, electrically conducting, in: Ullmann's Encycl. Ind. Chem., Wiley-VCH Verlag GmbH & Co. KGaA, Weinheim, Germany, 2000. https://doi.org/10.1002/14356007.a21_429.
[17] G. Inzelt, Conducting Polymers, Springer Berlin Heidelberg, Berlin, Heidelberg, 2012. https://doi.org/10.1007/978-3-642-27621-7.

[18] X. Zhang, J. Zhang, W. Song, Z. Liu, Controllable synthesis of conducting polypyrrole nanostructures, J. Phys. Chem. B. 110 (3) (2006) 1158–1165, https://doi.org/10.1021/jp054335k.
[19] S. Bose, T. Kuila, M.E. Uddin, N.H. Kim, A.K.T. Lau, J.H. Lee, In-situ synthesis and characterization of electrically conductive polypyrrole/graphene nanocomposites, Polymer (Guildf) 51 (25) (2010) 5921–5928, https://doi.org/10.1016/j.polymer.2010.10.014.
[20] M.A. Chougule, S.G. Pawar, P.R. Godse, R.N. Mulik, S. Sen, V.B. Patil, Synthesis and characterization of polypyrrole (PPy) thin films, Soft Nanosci. Lett. 01 (01) (2011) 6–10, https://doi.org/10.4236/snl.2011.11002.
[21] A.L. Pang, A. Arsad, M. Ahmadipour, Synthesis and factor affecting on the conductivity of polypyrrole: a short review, Polym. Adv. Technol. (2020) pat.5201, https://doi.org/10.1002/pat.5201.
[22] R. Ansari, Polypyrrole conducting electroactive polymers: synthesis and stability studies, E-J. Chem. 3 (4) (2006) 186–201, https://doi.org/10.1155/2006/860413.
[23] L.-X. Wang, X.-G. Li, Y.-L. Yang, Preparation, properties and applications of polypyrroles, React. Funct. Polym. 47 (2) (2001) 125–139, https://doi.org/10.1016/S1381-5148(00)00079-1.
[24] R.M.A.P. Lima, J.J. Alcaraz-Espinoza, F.A.G. da Silva, H.P. de Oliveira, Multifunctional wearable electronic textiles using cotton fibers with polypyrrole and carbon nanotubes, ACS Appl. Mater. Interfaces 10 (16) (2018) 13783–13795, https://doi.org/10.1021/acsami.8b04695.
[25] F. Gao, N. Zhang, X. Fang, M. Ma, Bioinspired design of strong, tough, and highly conductive polyol-polypyrrole composites for flexible electronics, ACS Appl. Mater. Interfaces 9 (7) (2017) 5692–5698, https://doi.org/10.1021/acsami.7b0071710.1021/acsami.7b00717.s00110.1021/acsami.7b00717.s00210.1021/acsami.7b00717.s00310.1021/acsami.7b00717.s004.
[26] N.M. Rowley, R.J. Mortimer, New electrochromic materials, Sci. Prog. 85 (3) (2002) 243–262, https://doi.org/10.3184/003685002783238816.
[27] J. Wang, C. Wu, P. Wu, X. Li, M. Zhang, J. Zhu, Polypyrrole capacitance characteristics with different doping ions and thicknesses, Phys. Chem. Chem. Phys. 19 (31) (2017) 21165–21173, https://doi.org/10.1039/C7CP02707A.
[28] W. Yuan, G. Han, Y. Xiao, Y. Chang, C. Liu, M. Li, Y. Li, Y. Zhang, Flexible electrochemical capacitors based on polypyrrole/carbon fibers via chemical polymerization of pyrrole vapor, Appl. Surf. Sci. 377 (2016) 274–282, https://doi.org/10.1016/j.apsusc.2016.03.114.
[29] F. Tavoli, N. Alizadeh, Optical ammonia gas sensor based on nanostructure dye-doped polypyrrole, Sensors Actuators B Chem. 176 (2013) 761–767, https://doi.org/10.1016/j.snb.2012.09.013.
[30] A. Ramanavičius, A. Ramanavičienė, A. Malinauskas, Electrochemical sensors based on conducting polymer—polypyrrole, Electrochim. Acta 51 (27) (2006) 6025–6037, https://doi.org/10.1016/j.electacta.2005.11.052.
[31] V. Ratautaite, G. Bagdziunas, A. Ramanavicius, A. Ramanaviciene, An application of conducting polymer polypyrrole for the design of electrochromic pH and CO 2 sensors, J. Electrochem. Soc. 166 (6) (2019) B297–B303, https://doi.org/10.1149/2.1221904jes.
[32] A. Talaie, J.Y. Lee, Y.K. Lee, J. Jang, J.A. Romagnoli, T. Taguchi, E. Maeder, Dynamic sensing using intelligent composite: an investigation to development of new pH sensors and electrochromic devices, Thin Solid Films 363 (1-2) (2000) 163–166, https://doi.org/10.1016/S0040-6090(99)00987-6.
[33] I. Sultana, M.M. Rahman, J. Wang, C. Wang, G.G. Wallace, H.-K. Liu, All-polymer battery system based on polypyrrole (PPy)/para (toluene sulfonic acid) (pTS) and polypyrrole (PPy)/indigo carmine (IC) free standing films, Electrochim. Acta 83 (2012) 209–215, https://doi.org/10.1016/j.electacta.2012.08.043.
[34] B. Yang, D. Ma, E. Zheng, J. Wang, A self-rechargeable electrochromic battery based on electrodeposited polypyrrole film, Sol. Energy Mater. Sol. Cells 192 (2019) 1–7, https://doi.org/10.1016/j.solmat.2018.12.011.
[35] Y. Kong, C. Wang, Y. Yang, C.O. Too, G.G. Wallace, A battery composed of a polypyrrole cathode and a magnesium alloy anode—toward a bioelectric battery, Synth. Met. 162 (7-8) (2012) 584–589, https://doi.org/10.1016/j.synthmet.2012.01.021.
[36] M.N. Akieh, S.F. Ralph, J. Bobacka, A. Ivaska, Transport of metal ions across an electrically switchable cation exchange membrane based on polypyrrole doped with a sulfonated calix[6]arene, J. Memb. Sci. 354 (1-2) (2010) 162–170, https://doi.org/10.1016/j.memsci.2010.02.052.
[37] M.N. Akieh, R.-M. Latonen, S. Lindholm, S.F. Ralph, J. Bobacka, A. Ivaska, Electrochemically controlled ion transport across polypyrrole/multi-walled carbon nanotube composite membranes, Synth. Met. 161 (17-18) (2011) 1906–1914, https://doi.org/10.1016/j.synthmet.2011.06.034.
[38] C. Li, H. Bai, G. Shi, Conducting polymer nanomaterials: electrosynthesis and applications, Chem. Soc. Rev. 38 (8) (2009) 2397, https://doi.org/10.1039/b816681c.
[39] I. Sultana, M.M. Rahman, J. Wang, C. Wang, G.G. Wallace, H.-K. Liu, Indigo carmine (IC) doped polypyrrole (PPy) as a free-standing polymer electrode for lithium secondary battery application, Solid State Ionics 215 (2012) 29–35, https://doi.org/10.1016/j.ssi.2012.03.034.
[40] C. Zhu, J. Zhai, D. Wen, S. Dong, Graphene oxide/polypyrrole nanocomposites: one-step electrochemical doping, coating and synergistic effect for energy storage, J. Mater. Chem. 22 (13) (2012) 6300, https://doi.org/10.1039/c2jm16699b.
[41] B.C. Thompson, S.E. Moulton, R.T. Richardson, G.G. Wallace, Effect of the dopant anion in polypyrrole on nerve growth and release of a neurotrophic protein, Biomaterials 32 (15) (2011) 3822–3831, https://doi.org/10.1016/j.biomaterials.2011.01.053.
[42] P. Jayamurgan, V. Ponnuswamy, S. Ashokan, T. Mahalingam, The effect of dopant on structural, thermal and morphological properties of DBSA-doped polypyrrole, Iran. Polym. J. 22 (3) (2013) 219–225, https://doi.org/10.1007/s13726-012-0119-x.
[43] M. Zhou, M. Pagels, B. Geschke, J. Heinze, Electropolymerization of pyrrole and electrochemical study of polypyrrole. 5. Controlled electrochemical synthesis and solid-state transition of well-defined polypyrrole variants, J. Phys. Chem. B 106 (39) (2002) 10065–10073, https://doi.org/10.1021/jp0210778.
[44] S. Kim, L.K. Jang, H.S. Park, J.Y. Lee, Electrochemical deposition of conductive and adhesive polypyrrole-dopamine films, Sci. Rep. 6 (2016) 30475, https://doi.org/10.1038/srep30475.
[45] M. Zhou, J. Heinze, Electropolymerization of pyrrole and electrochemical study of polypyrrole: 1. Evidence for structural diversity of polypyrrole, Electrochim. Acta 44 (11) (1999) 1733–1748, https://doi.org/10.1016/S0013-4686(98)00293-X.
[46] J. John, P. Saheeda, K. Sabeera, S. Jayalekshmi, Doped polypyrrole with good solubility and film forming properties suitable for device applications, Mater. Today Proc. 5 (10) (2018) 21140–21146, https://doi.org/10.1016/j.matpr.2018.06.512.
[47] N. Su, Improving electrical conductivity, thermal stability, and solubility of polyaniline-polypyrrole nanocomposite by doping with anionic spherical polyelectrolyte brushes, Nanoscale Res. Lett. 10 (2015) 301, https://doi.org/10.1186/s11671-015-0997-x.
[48] E. Håkansson, T. Lin, H. Wang, A. Kaynak, The effects of dye dopants on the conductivity and optical absorption properties of polypyrrole, Synth. Met. 156 (18–20) (2006) 1194–1202, https://doi.org/10.1016/j.synthmet.2006.08.006.
[49] E.M. Girotto, M.-A. De Paoli, Polypyrrole color modulation and electrochromic contrast enhancement by doping with a dye, Adv. Mater. 10 (1998) 790–793, https://doi.org/10.1002/(SICI)1521-4095(199807)10:10<790::AID-ADMA790>3.0.CO;2-R.
[50] E.M. Girotto, W.A. Gazotti, C.F. Tormena, M.-A. De Paoli, Photoelectronic and transport properties of polypyrrole doped with a dianionic dye, Electrochim. Acta 47 (9) (2002) 1351–1357, https://doi.org/10.1016/S0013-4686(01)00857-X.
[51] J. Ferreira, M.J.L. Santos, R. Matos, O.P. Ferreira, A.F. Rubira, E.M. Girotto, Structural and electrochromic study of polypyrrole synthesized with azo and anthraquinone dyes, J. Electroanal. Chem. 591 (1) (2006) 27–32, https://doi.org/10.1016/j.jelechem.2006.03.016.
[52] F. Tavoli, N. Alizadeh, In situ UV–vis spectroelectrochemical study of dye doped nanostructure polypyrrole as electrochromic film, J. Electroanal. Chem. 720–721 (2014) 128–133, https://doi.org/10.1016/j.jelechem.2014.03.022.
[53] L.F. Loguercio, C.C. Alves, A. Thesing, J. Ferreira, Enhanced electrochromic properties of a polypyrrole–indigo carmine–gold nanoparticles nanocomposite, Phys. Chem. Chem. Phys. 17 (2) (2015) 1234–1240, https://doi.org/10.1039/C4CP04262J.
[54] M. Bayat, H. Izadan, B.G. Molina, M. Sánchez, S. Santiago, D. Semnani, M. Dinari, G. Guirado, F. Estrany, C. Alemán, Electrochromic self-electrostabilized polypyrrole films doped with surfactant and azo dye, Polymers (Basel) 11 (2019) 1757, https://doi.org/10.3390/polym11111757.
[55] D. Aradilla, J. Casanovas, F. Estrany, J.I. Iribarren, C. Alemán, New insights into the characterization of poly(3-chlorothiophene) for electrochromic devices, Polym. Chem. 3 (2) (2012) 436–449, https://doi.org/10.1039/C1PY00504A.
[56] A.M. Österholm, D.E. Shen, J.A. Kerszulis, R.H. Bulloch, M. Kuepfert, A.L. Dyer, J. R. Reynolds, Four shades of brown: tuning of electrochromic polymer blends toward high-contrast eyewear, ACS Appl. Mater. Interfaces 7 (3) (2015) 1413–1421, https://doi.org/10.1021/am507063d.
[57] S. Zhang, G. Sun, Y. He, R. Fu, Y. Gu, S. Chen, Preparation, characterization, and electrochromic properties of nanocellulose-based polyaniline nanocomposite films, ACS Appl. Mater. Interfaces 9 (19) (2017) 16426–16434, https://doi.org/10.1021/acsami.7b02794.
[58] S.S. Kalagi, S.S. Mali, D.S. Dalavi, A.I. Inamdar, H. Im, P.S. Patil, Limitations of dual and complementary inorganic–organic electrochromic device for smart window application and its colorimetric analysis, Synth. Met. 161 (11-12) (2011) 1105–1112, https://doi.org/10.1016/j.synthmet.2011.03.028.
[59] Y.A. Udum, A. Durmus, G.E. Gunbas, L. Toppare, Both p- and n-type dopable polymer toward electrochromic applications, Org. Electron. 9 (4) (2008) 501–506, https://doi.org/10.1016/j.orgel.2008.02.009.
[60] S. Tarkuc, E.K. Unver, Y.A. Udum, L. Toppare, Multi-colored electrochromic polymer with enhanced optical contrast, Eur. Polym. J. 46 (11) (2010) 2199–2205, https://doi.org/10.1016/j.eurpolymj.2010.08.002.
[61] R. Lakshmanan, P.P. Raja, N.C. Shivaprakash, S. Sindhu, Fabrication of fast switching electrochromic window based on poly(3,4-(2,2-dimethylpropylenedioxy)thiophene) thin film, J. Mater. Sci. Mater. Electron. 27 (6) (2016) 6035–6042, https://doi.org/10.1007/s10854-016-4527-0.